Science of the Total Environment 946 (2024) 174102

Contents lists available at ScienceDirect

Science of the Total Environment

journal homepage: www.elsevier.com/locate/scitotenv

Drivers of barrier island water-table fluctuations and groundwater salinization

Ryan S. Frederiks [a,1], Anner Paldor [a], Lauren Donati [a], Glen Carleton [b], Holly A. Michael [c,*]

[a] University of Delaware Department of Earth Sciences, Newark, DE, USA
[b] MidAtlantic Geophysics LLC, USA
[c] University of Delaware Department of Earth Sciences and Department of Civil and Environmental Engineering, Newark, DE, USA

HIGHLIGHTS

- Monitored groundwater levels and salinity on three barrier islands
- Tested influence of recharge, storm-surge overwash, tides, and waves
- More exposed barrier islands were influenced by more drivers.
- Surface-water connectivity and topography caused differences in driver influence.
- High hydraulic conductivity and high storage caused longer lasting salinization.

GRAPHICAL ABSTRACT

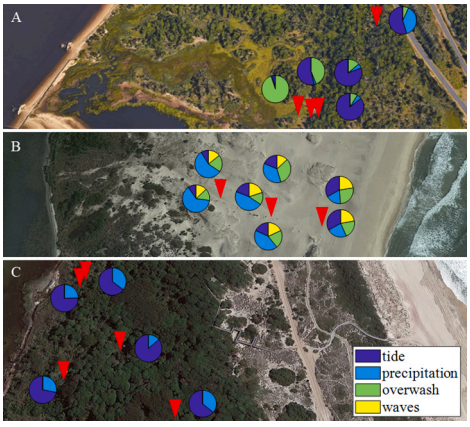

ARTICLE INFO

Editor: JV Cruz

Keywords:
Coastal groundwater
Saltwater intrusion
Salinization
Barrier islands
Storm-surge overwash
Groundwater-surface water interactions

ABSTRACT

Barrier islands are threatened by climate change as sea-level rise and higher frequency storm surge lead to more flooding and saltwater intrusion. Vegetation plays a vital role in preventing erosion of barrier islands due to aeolian and hydrological forces. However, vegetation on barrier islands is threatened by rising water tables causing hypoxic conditions and storm-surge overwash introducing saline water to the root zone. To better protect barrier island ecosystems, it is critical to identify the relative influence of different hydrological drivers on water table elevation and salinity, and understand how this influence varies spatially and temporally. In this study, three barrier island sites were instrumented with groundwater wells monitoring water level and specific conductance. Using these data, a set of transfer function noise models were calibrated and used to determine the relative influence of hydrologic drivers including precipitation, evapotranspiration, bay and ocean water levels, and wave height on groundwater levels and specific conductance. We found that drivers of water-level change and specific conductance vary strongly among sites, depending primarily on the surface water connectivity and

* Corresponding author.
E-mail addresses: rsfreder@udel.edu (R.S. Frederiks), annerpal@udel.edu (A. Paldor), ldonati@udel.edu (L. Donati), glen@midatlanticgeophysics.com (G. Carleton), hmichael@udel.edu (H.A. Michael).
[1] Present address: Temple University, Department of Earth and Environmental Science.

https://doi.org/10.1016/j.scitotenv.2024.174102
Received 6 March 2024; Received in revised form 14 June 2024; Accepted 16 June 2024
Available online 20 June 2024

the geology of the island. Sites with close connection to inlets showed more salinization and responded to a larger number of drivers, while sites that were poorly connected to the ocean responded to fewer drivers.

1. Introduction

Barrier islands are dynamic sediment deposits that are especially vulnerable to sea-level rise, storm surge, and decreased sediment supply from anthropogenic interruptions of longshore drift (Ceia et al., 2010). Barrier islands form when sea levels rise and fill low lying topography landward of the previous coastline (Hoyt, 1967), or from landward movement of sand bars (Otvos, 1981; Otvos and Carter, 2013). While barrier islands only cover a small portion of the world's coastlines (Stutz and Pilkey, 2001), they perform important ecosystem services by protecting coastal areas from storm-surge inundation and dissipating wave energy (Stone et al., 2005). For example, Corpus Christi, Texas, USA could experience up to 70 % more hurricane flooding by 2030 due to the deterioration of barrier islands (Irish et al., 2010). Barrier islands are naturally dynamic systems that migrate in response to sea-level rise, changing sediment supply and storm surge overwash. Overwash deposits sediment from the beach into the back-barrier marsh causing the island to migrate landward. The persistence of barrier islands in response to these threats depends on coastal processes such waves and storm surge, but also strongly on the ecological communities present.

Barrier island ecosystems strongly affect the resilience/resistance of each island. The migration of barrier islands in response to sea level rise and storm surge is controlled by where the island falls on the continuum of resistance and resilience. High resistance systems have higher elevation and more woody plants that prevent erosion. While these systems resist storm-surge overwash, the island is unable to migrate quickly and can be in danger of becoming submerged by rising sea levels. On the other hand, high resilience systems have lower topography and more overwash-tolerant species. These systems are capable of rapid migration in the face of changing sea levels (Anthony Stallins and Corenblit, 2018; Stallins, 2005; Stallins and Parker, 2003; Zinnert et al., 2016, 2017, 2019). High resistance systems are more effective at mitigating onshore impact of storm surge, but they are also more at risk of disappearing if sea-level rise exceeds the pace at which they can migrate towards the mainland. To understand how barrier islands will be impacted by climate change, it is critical to understand how barrier island ecosystems will evolve in response to changing hydrological forcing.

Barrier island ecosystems are dependent on the existence of fresh groundwater, and are susceptible to changes in groundwater specific conductance and thickness/water content of the unsaturated zone. Many woody species found in dune swales are highly susceptible to changes in specific conductance caused by storm-surge flooding (Tolliver et al., 1997; Young et al., 1994). Other studies have found a relationship between groundwater specific conductance and vegetation patterns (Holt et al., 2017). Additionally, vegetation is susceptible to changes in water table elevation, as high water tables can cause mortality if the root zone is not oxygenated (van der Valk et al., 1994). Overwash events cause vegetation mortality due to salinization, especially among seedlings, whereas sea-level rise increases mortality for mature trees close to the shoreline or in low-lying areas that experience higher water tables and limited vadose zone thickness (Kearney et al., 2019). Thus, to understand how barrier island ecosystems will change in the future it is necessary to understand how the hydrological forcings acting on barrier islands will alter the specific conductance and water-table elevation of barrier-island groundwater.

In addition to the ecological impacts of sea-level rise and storm surge on barrier islands, many people depend on barrier island groundwater as their primary drinking water supply. About 1.4 million people live on barrier islands in the U.S., and barrier islands have experienced substantial population growth over the last few decades (Zhang and Leatherman, 2011). Barrier islands also reduce storm-surge heights in the back bay (Bilskie et al., 2016), thus protecting the shorelines behind them and the water supply for approximately 20 million people in the mid-Atlantic who utilize groundwater resources (Masterson et al., 2013).

Barrier island ecosystems and water resources will be threatened in the near future from the effects that both sea-level rise and more intense and frequent coastal storms have on their groundwater systems. Many studies have investigated groundwater vulnerability to sea-level rise induced salinization (e.g. Chang et al., 2019; Lobo-Ferreira et al., 2005; Morgan and Werner, 2014; Werner et al., 2012) and rising water tables (Befus et al., 2020; Rahimi et al., 2020; Rotzoll and Fletcher, 2013). Far fewer have investigated vulnerability to storm surge overwash. Storm surges are expected to intensify due to climate change because the range of hurricane formation will move northward (Studholme et al., 2021), and sea-level rise will cause storm return levels to be higher (Garner et al., 2017). Shorter return periods for large storms will impair water quality in coastal aquifers. Aquifer vulnerability to storm-surge salinization is dependent on both topography (Yu et al., 2016) and aquifer properties (Yang et al., 2018). Highly connected topography causes a greater volume of the aquifer to be salinized. On the other hand, surface depression storage, i.e. poorly connected low topography systems infiltrate a higher volume of salt, but require larger storms to overtop (Yu et al., 2016). Yang et al. (2018) also showed that aquifers with low horizontal to vertical hydraulic conductivity ratios (Kx/Kz) and low recharge rates were the most vulnerable to storm-surge induced salinization. (Mahmoodzadeh and Karamouz, 2019), showed that heterogeneity did not have a significant effect on the volume of aquifer salinized compared to homogeneous aquifers and flushing occurred within a year with some density fingers lasting up to ten years. Storm surges will also cause water tables to rise inland, resulting in groundwater flooding (Housego et al., 2021). While these results suggest that certain types of barrier islands are more vulnerable than others, it is not clear how drivers of water table change and salinization due to sea-level rise and storm-surge overwash vary within and among barrier islands.

Field measurements have shown that overwash-induced salinization occurs around the world (Anderson Jr., 2002; Anderson Jr. and Lauer, 2008; Cardenas et al., 2015; Huizer et al., 2017; Illangasekare et al., 2006). Pacific atolls are particularly vulnerable to salinization from storm-surge overwash as shallow groundwater is often the only source of freshwater available. Oberle et al. (2017) showed that specific conductance on a Pacific atoll recovered to the background level about one month after an overwash event, and precipitation and tides were also shown to have an effect on groundwater specific conductance. While these hydrological processes all influence the specific conductance of coastal aquifers, few studies have quantified the relative influence of each of these drivers and how they vary across both distance from the shoreline and barrier island typology. Further, few studies have conducted long-term monitoring of barrier island water levels and specific conductance to capture the range of hydrologic drivers and their effects on groundwater.

In this study, water level and specific conductance data were collected in multiple wells that span the transition from beach to upland at three different barrier islands along the mid-Atlantic coastline of the USA, representing a diverse array of ecological characteristics but similar geological characteristics. Time series models were fit to observation data in each well to quantify the relative influence of different drivers, and the drivers were compared to understand regional-scale groundwater vulnerability.

The objective of this study was to quantify the primary drivers of both water level and specific conductance on barrier islands and to

evaluate the hypothesis that storm surge causes greater saltwater intrusion than other processes such as tidal fluctuations. To achieve this, we.measured groundwater levels and specific conductance over a range of hydrologic regimes including multiple storm surge events, and applied data-driven models to identify drivers at three field sites over space and time. Using these data, we can begin to understand the how barrier island vulnerability to sea-level rise and storm surge overwash varies spatially and temporally.

2. Study sites/methods

2.1. Overview

To understand the primary drivers of barrier-island water table change and salinization, three sites were instrumented with conductivity, temperature and depth loggers in nine wells at Assateague Island, Maryland (MD); five wells at Sandy Hook, New Jersey (NJ); and five

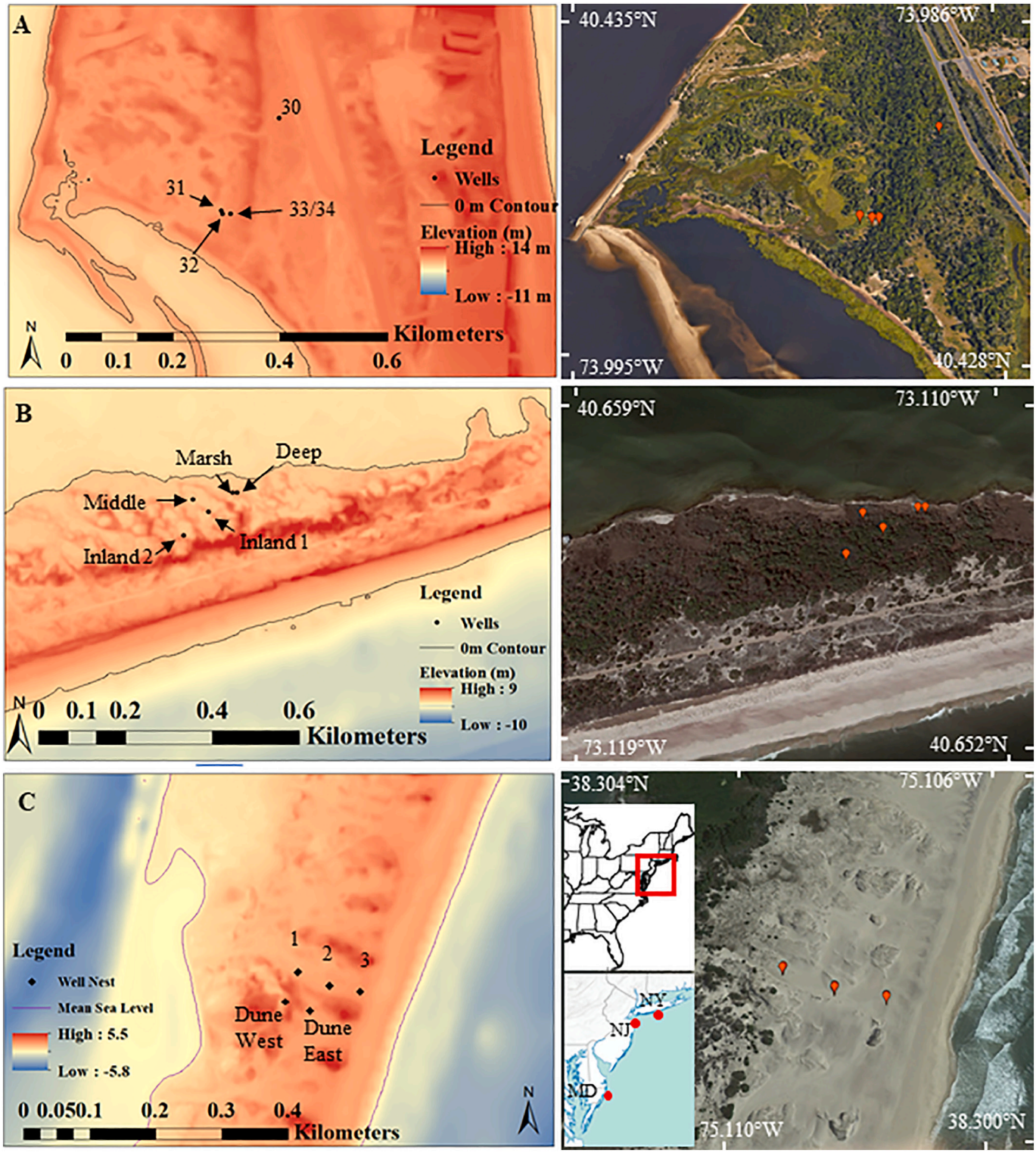

Fig. 1. Map of well locations and land surface elevation for A) Sandy Hook, NJ B) Fire Island, NY, and C) Assateague Island, MD.

wells at Fire Island, New York (NY). Hydraulic head, specific conductivity, and temperature were measured at 5, 6, or 15-min intervals depending on the site. Head measurements were corrected for barometric pressure and specific conductivity measurements were converted to specific conductance at 25 °C based on the temperature. Additional data including precipitation, tide level, wave height, and evapotranspiration were collected from other sources for each of the sites.

2.2. Sandy Hook National Gateway, NJ

Sandy Hook is a peninsula located at the mouth of New York harbor that was created by longshore transport of beach sand into the bay (Stanford et al., 2015). It consists of Quaternary beach and estuarine sand and mud overlying Cretaceous sedimentary deposits (Johnson et al., 2018). All wells at Sandy Hook were installed and instrumented by the United States Geological Survey (USGS) and the data can be found at site numbers 402548073592301 (well 31), 402548073592302 (well 32), 402548073592303 (well 33), 402548073592304 (well 34), and 402554073591901 (well 30) (Fig. 1A). Well depths for wells 30, 31, 32, and 33 ranged from 1.3 to 1.7 m while the depth for well 34 was 6.3 m. Four of the wells (Well 31, 32, 33, 34) were located in a transect from marsh to forest on the bay side of the peninsula while the final well (well 30) was located approximately 190 m inland and does not typically experience overwash. Additional data obtained for Sandy Hook include tidal levels, precipitation, and evapotranspiration.

For Sandy Hook, a tidal time series was obtained from NOAA tide gauge 8531680. Because the Sandy Hook bay is well connected to the ocean, the tide gauge measurement was assumed to capture water levels on both sides of the peninsula. A wave time series was created using wind speed measured at the NOAA tide gauge. First, all wind coming from the east (1 to 180°) was excluded from the dataset. This is because the barrier spit protects the wells from wind-driven waves coming from the east. Then the wind speed was converted to wave height using the equation for fetch-limited waves (Coastal Engineering Research Center, 1984). Fetch length was measured in google earth every 30° and the wind direction time series was converted into a fetch length time series. This was input into the fetch-limited wave equation to produce a wave time series. An overwash time series was created by removing all tide measurements below the land surface elevation at each of the well locations. The precipitation time series was obtained from NOAA station WBAN:54760 located at the Belmar Farmingdale Allaire Airport, NJ. Wind speed, temperature, dewpoint temperature, and solar radiation data were obtained from the National Solar Radiation Database (NSRDB) to calculate evapotranspiration using the Penman-Montieth method (Allen et al., 1998). This method estimates the reference evapotranspiration based on climatic parameters including temperature, relative humidity, wind speed, and solar radiation, and it approximates reference evapotranspiration from grass.

2.3. Fire Island, NY

Fire island consists of unconsolidated Holocene and Pleistocene sediments above a clay confining unit (Schubert, 2010). The Holocene sediments, which the surficial aquifer is composed of, consist of lagoonal deposits, estuarine mud, seagrass beds, peat deposits and barrier island sands (Schubert 2010). Five wells were installed by the USGS with well numbers of 403922073064401 (marsh well), 403922073064402 (deep marsh well), 403921073064801 (middle well), 403921073070401 (inland well 1), 403919073064801 (inland well 2). Well depths range from 2.3 m to 3.9 m.

There were two wells located in the marsh (marsh and deep wells), one on the edge of the marsh (middle well) and two more located inland (inland 1 and inland 2 wells) (Fig. 1B). The wells were installed on the back-bay side of the island which means they were not well connected to the ocean. A time series of bay water levels was obtained from the USGS gage 01305575 in the Great South Bay at Watch Hill. An ocean time series was obtained from the Sandy Hook tide gage (8531680). A wave time series was created using windspeed measured at NOAA buoy 44069 in the Great South Bay, and an overwash time series was produced by removing all points where bay levels were below the land-surface elevation of the well. A precipitation time series was obtained from a NOAA station WBAN: 04781 at the Macarthur Airport in Islip, NY. Wind speed, temperature, dewpoint temperature, and solar radiation data were obtained from the National Solar Radiation Database (NSRDB) to calculate evapotranspiration using the Penman-Montieth method.

2.4. Assateague Island, MD

Assateague is a barrier island located on the eastern shore of Maryland and Virginia. The island consists of Holocene beach sand overlying lagoonal sandy mud. Seven wells were installed in a transect that runs between two dunes and two additional wells were located in the dunes to the south of the transect (Fig. 1C). Each transect well was 0.051 m diameter stainless steel with a 0.3-m well screen at the bottom of the well. Sensors were placed in the center of the screened section. The depths of each sensor below land surface were variable due to dynamic erosion and deposition, but ranged from approximately 1.6 m to 4.1 m at the time of installation. Four of the wells were installed and instrumented by the USGS for this study. Data for wells 2 and 3 shallow can be found under site numbers 381806075063301 and 381806075063201 respectively while data for the two dune wells can be found under site numbers 381804075063402, and 381805075063502. Wells 1 deep, 1 shallow, 2 deep, 2 middle, and 3 deep were installed and instrumented for this study. The wells are located on the northern end of the island which has been eroding due to the effects of dredging the Ocean City inlet, which prevents deposition of sediment moving southwards that would replenish the northern part of Assateague. Thus, the wells on Assateague are very susceptible to overwash events which occur regularly from the ocean side. Additional data was collected on all expected drivers of water level and specific conductance change including tidal levels, precipitation, evapotranspiration, wave height and overwash.

Bay water levels were obtained from NOAA tide gage located at the Ocean City Inlet (Station ID: 8570283). Precipitation data was obtained from the NOAA hourly global precipitation database at the Ocean City Municipal Airport (Station ID: 74594693786). Ocean-side wave height was obtained from a NOAA buoy located 26 nautical miles southeast of Cape May, NJ (Station ID: 44009). Wind speed, temperature, dewpoint temperature, and solar radiation data were obtained from the National Solar Radiation Database (NSRDB) to calculate evapotranspiration using the Penman-Montieth method. An estimate of overwash events was created by using the Digital Elevation Model (DEM) for Assateague obtained from the NOAA National Center for Environmental Information Continuously updated DEM at the 1/9th arc second resolution. Time periods where the bay elevation exceeded the maximum land surface elevation between the well and the bay were selected from the bay time series, and for all other times the overwash time series was set to zero. A similar procedure was used to create the ocean overwash timeseries except the ocean elevation was estimated by adding the observed water level in the bay with the observed wave height at the ocean buoy corrected to a runup estimate (Stockdon et al., 2006). There was a data gap in the wave height from 5/31/2021 to 7/1/2021 that was filled in with the average of the wave time series. Additionally, wave height measurements from buoy Station OCSM2, which is closer to shore, were not used because the dataset does not span the time frame covered by the well data. However, this buoy shows a much lower wave height than the buoy further offshore that was used in this analysis. Thus, the number and level of overwash events might be overestimated here.

2.5. Site comparison

Pendleton et al. (2004a) showed that Assateague is highly vulnerable to sea-level rise as measured by the geomorphology, shoreline erosion,

surface slope, significant wave height, tidal range, and measured rate of sea-level rise. Similarly, Fire Island is highly vulnerable due to its shallow slope and geomorphology, but it has only moderate erosion occurring (Pendleton et al., 2004b). Finally, Sandy Hook is relatively invulnerable due to its higher slope and lower erosion rate (Pendleton et al., 2005). Assateague is migrating landward and Fire Island is eroding into the Great South Bay, while Sandy Hook is expanding into the Sandy Hook bay. Each site has experienced ecosystem changes. Fire Island and Sandy Hook have experienced increased mortality in old growth holly forests hypothesized to be caused by sea-level rise (Raphael, 2014) and/or storm-surge overwash (Stalter and Heuser, 2015). While Fire Island currently has the capacity to recover from periodic overwash events (Kilheffer et al., 2019), increased frequency and intensity of storm surge expected from sea-level rise (Tebaldi et al., 2012) likely will alter vulnerability in the future. Similarly, Assateague experienced a die off in its pine forest due to a pine beetle infestation that was potentially exacerbated by saltwater intrusion (Asaro et al., 2017).

2.6. Time series models

Given the sparsity of geological data for model calibration and the data density, time series models were chosen to estimate the relative influence of drivers at each site. Bakker and Schaars (2019) have suggested that data-driven time series models are often simpler than physics-based numerical models and fit data better. Transfer function noise models (TFN) and cross correlation were used to quantify the relative impact of different drivers on the intensity and persistence of water level and specific conductance changes for all wells. Transfer function noise models have been used for a variety of purposes including identifying drought conditions (Brakkee et al., 2022), and estimating landslide risk due to high groundwater levels (Uwihirwe et al., 2022). These models fit simple functions including gamma and exponential functions to a set of input time series to produce the target output time series. Transfer function noise models were fit to the hydraulic head data at each well using tide, wave, overwash, precipitation, and evapotranspiration data as inputs with a Python package called Pastas (Collenteur et al., 2019).

Prior to analysis, data processing was done on both input time series (tides, waves, precipitation, evapotranspiration, overwash, and the output time series (heads). Each input time series was resampled to an hourly timestep by choosing the closest sampling point to each hour and daily timesteps by averaging. Data gaps in the input time series can cause a faulty calibration of the TFN models. Thus, the output time series were filtered to a timeframe where all the input time series were available or where the data gaps were small enough (less than a few hours) such that they could be interpreted with linear interpolation for the tides, waves, evapotranspiration, and overwash or set to zero for the precipitation. Different combinations of input stressors and input functions for each stressor were tested. Additionally, in some cases, the recharge function in Pastas was used while in other cases precipitation and evapotranspiration were added to the model separately. Stressors that worsened model fit or had limited effect were removed for all wells at a given site. This process occurred iteratively until a reasonable fit was found for each well. Once an acceptable fit was achieved ($R^2 > 0.7$), the stressors were separated out into their individual contributions to the hydraulic head at each site. Ideally, a similar approach could be used for understanding the drivers of specific conductance; however, transfer function models calibrated to specific conductance data had very poor model fits. This is due to complicated processes governing the specific conductance response to hydrological changes. TFN models assume that a stressor has the same directional impact on the output time series, while this is not always the case for the specific conductance. For example, overwash can both salinize and freshen groundwater. When an overwash occurs, it can push the freshwater-saltwater interface deeper thus freshening a well located in the saltwater portion, but it can also salinize the well on a longer timescale. Thus, a different approach was needed to understand the impacts of different hydrological drivers on specific conductance changes.

Cross correlation was used to discover whether the specific conductance was correlated to changes in any of the drivers. Cross correlation is a quantitative measurement of the relationship between two timeseries at different time lags. The maximum value of the cross correlation is 1, indicating that the two timeseries are perfectly correlated at the given lag time and the minimum is −1, indicating they are perfectly inversely correlated at that lag. A cross-correlation value below the 95 % confidence interval suggests that the timeseries are not related. Because flushing saltwater out of the aquifer is expected to take longer than the water level increase in both the ocean and at the water table, the cross-correlation between specific conductance and these processes is expected to be low. To understand the impact of each of the different drivers on the specific conductance, cross-correlation between specific conductance and each of the input drivers (tides, waves, overwash, precipitation, and evapotranspiration) was performed from 1-h to 1-month lags at each well. The specific conductance and all other driver time series were resampled to 1-h timesteps and all data gaps were linearly interpolated.

3. Results

3.1. Sandy Hook, NJ:

3.1.1. Overview

Sandy Hook showed a gradient in the impact of overwash from the marsh to the forest, with the marsh wells experiencing substantial overwash and the forest wells experiencing less frequent overwash. Well 31 was located in the marsh and experienced overwash daily. This led to relatively high specific conductance that did not fall below 50 % seawater concentration (Fig. 2A). Moving inland, well 32 experienced relatively frequent inundation, but had time to recover to a background specific conductance of 15–20 mS/cm (Fig. 2B). Well 33 experienced even less overwash than both wells 31 and 32 and was able to fully recover to freshwater concentrations after most overwash events (Fig. 2C). Finally, well 34 was screened in the freshwater-saltwater interface, and experienced increases in the specific conductance from some events but generally these increases were small, and the specific

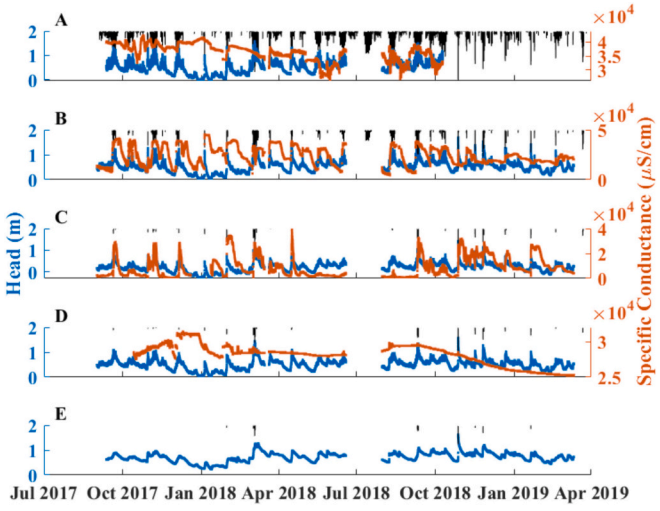

Fig. 2. Well measurements from Sandy Hook, NJ. Hydraulic head and predicted overwash events (black lines) in meters above NAVD88 on the left axis and specific conductance in μS/cm on the right axis with increasing distance from the shore for A) Well 31 (marsh well), B) Well 32 (transition well), C) Well 33 (forest well), D) Well 34 (deep well, collocated with well 33), and E) Well 30 (inland well).

conductance declined from September 2018 to March 2019 (Fig. 2D). Well 30 was located farther inland and specific conductance was not measured in this well; however, the tidal elevations exceeded the land surface elevation a few times over the monitoring period (Fig. 2E). There was a single event where water levels rose rapidly on October 26–27, 2018 suggesting a possible overwash event.

A change occurred in the specific conductance time series in September 2018. Prior to that, after each overwash event, both wells 32 and 33 typically returned to their pre-overwash levels. However, beginning in August 2018 neither well returned to its initial specific conductance after overwash events (Fig. 2B, C). On the other hand, well 34 saw a steady decline in specific conductance beginning in late September 2018 (Fig. 2D). However, there was no observable change in the drivers for the water levels in each of these wells.

3.1.2. Water level change (TFN models)

To understand the influence of different drivers on the water levels, they were modeled with a combination of tidal level, wave height, precipitation, evapotranspiration, and overwash. The results show that water levels at Sandy Hook were primarily driven by overwash events, precipitation, and tidal levels (Fig. 3). Model fits at Sandy Hook ranged from an R^2 of 0.73 to 0.85 with a root mean squared error (RMSE) of 0.08 to 0.11 m (Table 1). Water level fluctuations for well 31 were primarily controlled by overwash events and seasonal tidal fluctuations, while precipitation had a modest effect on the heads (a maximum of ~0.22 m) (Fig. 3A). Daily tidal oscillations had minimal effect on the water levels (<0.05 m of change), but seasonal changes in tidal elevation had a greater effect on water levels (0.5 m of change). Overwash occurred multiple times per month and the water level often did not recover before another overwash event occurred; however, overwash occurred in clusters followed by periods with few overwash events (e.g. December 2017). Overwash contributed a maximum of 1 m of head change at well 31, but even small overwash events increased heads by 0.1 m. Further inland, well 32 experienced overwash events approximately 1–2 times per month, and had longer periods without overwash influence (Fig. 3B). Well 32 had a higher daily tidal oscillation than well 31 (~0.05 m) and a greater seasonal tidal oscillation (~0.68 m). Heads in well 32 were impacted by precipitation similarly to well 31 with a maximum of ~0.26 m of head change. Well 33 and 34 had only a few overwash events (Fig. 3C, D). These wells had similar daily tidal fluctuations to well 32 (~0.05 m), but the largest seasonal change due to tidal fluctuations (0.86 and 0.92 respectively). Precipitation had a slightly higher impact on wells 33 and 34 than well 32 and contributed a maximum of 0.3 m of head change. Well 30 showed the strongest influence of precipitation with a maximum contribution of 0.4 m and a moderate contribution of seasonal tidal fluctuations (~0.6 m) compared to wells 31, 32, 33 and 34 (Fig. 3E). Well 30 displayed no contribution from daily tidal fluctuations, and a single overwash event that took about 3 months to recover from (Fig. 3E).

Table 1
Transfer function noise model fit.

	Daily R^2	Daily RMSE (m)	Hourly R^2	Hourly RMSE (m)
Sandy Hook				
Well 30	0.84	0.08	0.85	0.08
Well 31	0.73	0.13	0.82	0.1
Well 32	0.72	0.12	0.77	0.11
Well 33	0.73	0.11	0.75	0.11
Well 34	0.7	0.11	0.73	0.11
Fire Island				
Marsh Well	0.83	0.06	0.83	0.09
Deep Well	0.87	0.06	0.75	0.12
Middle Well	0.8	0.05	0.76	0.06
Inland Well 1	0.91	0.03	0.92	0.03
Inland Well 2	0.84	0.07	0.79	0.05
Assateague				
Well 1 Shallow	0.78	0.07	0.75	0.08
Well 1 Deep	0.77	0.07	0.78	0.07
Well 2 Shallow	0.9	0.05	0.9	0.05
Well 2 Middle	0.74	0.08	0.78	0.08
Well 2 Deep	0.76	0.08	0.52	0.11
Well 3 Shallow	0.82	0.08	0.86	0.07
Well 3 Deep	0.7	0.1	0.7	0.11
Dune Well 1	0.9	0.05	0.79	0.07
Dune Well 2	0.87	0.06	0.88	0.06

3.1.3. Specific conductance change (cross-correlation)

There was a correlation between overwash events and specific

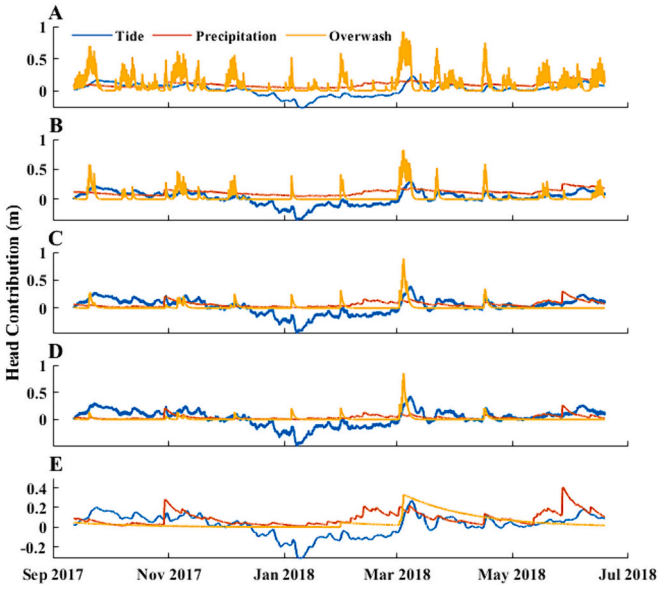

Fig. 3. Transfer function noise models for Sandy Hook, NJ broken down by the influence of tide, precipitation, and overwash drivers for A) Marsh well 31, B) Transition well 32, C) Upland well 33, D) Deep well 34, and E) Inland well 30.

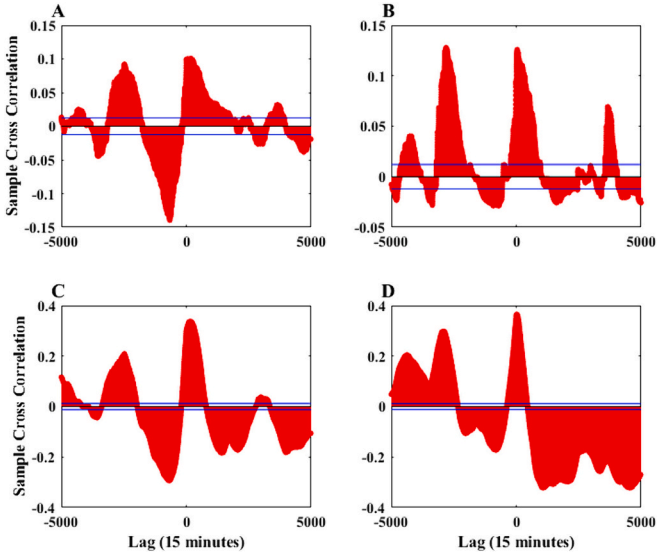

Fig. 4. Relationship between specific conductance, overwash, and head at lag times from −1250 to 1250 h for Sandy Hook, NJ. When the cross correlation is above/below the blue lines, it indicates a *p*-value of <0.05. A) Correlation of specific conductance and overwash in well 32. B) Correlation of specific conductance and overwash in well 33. C) Correlation of specific conductance and head in well 32. D) Correlation of specific conductance and head in well 33.

conductance changes for wells 32 and 33 (Fig. 4). The maximum correlation was approximately 10 % at lags of 6 h and 51 h for well 32 (Fig. 4A), and 12.5 % with a lag of 41 h for well 33 (Fig. 4B). The peak correlation occurred twice for well 32 likely because the overwash is tidal, i.e. for each salinization event there were multiple overwash events as the tide went in and out multiple times. The upper well had fewer overwash events because only the highest tide overwashed that well. Thus, the specific conductance peaked approximately 6 h after an overwash event in well 32 and then peaked again 51 h later as more overwash occurred. On the other hand, wells 31 and 34 exhibited no correlation between overwash and specific conductance. Wells 32 and 33 also showed a weak positive correlation between specific conductance and the tides, whereas wells 31 and 34 showed a negative correlation. None of the wells showed a correlation between specific conductance and precipitation.

3.2. Fire Island, NY

3.2.1. Overview

Fire Island groundwater was generally fresh both in the marsh and in the upland, and overwash played a limited role in changing the specific conductance. For both the marsh and deep wells there are no predicted overwash events as the bay water levels never exceed the land surface elevation at these wells. Despite the fact that no overwash is predicted based on the data, there are specific conductance spikes at both the marsh and deep wells (Fig. 5A, B). The middle well was predicted to have a substantial number of overwash events; however, no specific conductance data was collected in this well. Errors in overwash prediction could be due to error in the surveyed elevations; however, both survey elevations from the USGS and the NOAA DEM suggest that the tidal elevation never exceeds the land-surface elevation at the wells. Thus, there are potentially shorter scale wind-driven waves or seiches within the Great South Bay that drive the observed salinization events. Based on the measured specific conductance and hydraulic head spikes, few overwash events occurred in the marsh, and they were fully flushed out between events. The overwash events salinized the shallow well to a maximum of ~10,000 μS/cm or 20 % of seawater concentration (Fig. 5A) and the deep well to 10 % of seawater concentration (Fig. 5B). This suggests that a smaller volume of saline water entered the aquifer during overwash events than at Sandy Hook as the bay water at Fire Island typically fluctuated between 35,000–50,000 μS/cm, or 70–100 % seawater salinity. The deep well usually had a damped and lagged response to salinization events compared to the shallow well; however, one of the overwash events in the shallow well (September 20th 2017) was not present in the deeper well. The damped change in specific conductance observed in the deeper well was likely due to dispersion and dilution of the salt pulse from the overwash, with the lag suggesting a low vertical hydraulic conductivity. Fire Island experienced relatively few overwash events during the study period likely because the bay is sheltered from large waves and water levels near the wells take a long time to respond to changes occurring on the ocean side of the island. The inland wells saw almost no change in specific conductance and remained fresh, suggesting that overwash events are rare for the inland wells.

3.2.2. Water level change (TFN models)

Fire Island water levels were modeled using the ocean level, bay level, precipitation, evapotranspiration, bay wave height and overwash. The changes in water level were dominantly driven by the tidal elevation in the bay and the recharge (Fig. 6). As ocean level, bay wave height and overwash negatively impacted model fits, they were removed from the models. Models were also resampled to daily timesteps with the mean due to poor model fits for hourly timesteps. Poor fits at the hourly timestep are probably due to the poor constraints on short term drivers such as overwash and short-term wind-driven waves. Model fits ranged from an R^2 of 0.8 to 0.91 and an RMSE of 0.03 to 0.07 m having the best model fit of all the sites (Table 1). Water levels in the marsh and deep wells responded quickly to recharge increasing up to a maximum of 0.3 m, but the impact of recharge dissipated rapidly (within 1 day) (Fig. 6A, B). The middle well declined slower than the marsh and deep wells taking 1–2 weeks to recover (Fig. 6C), but declined rapidly within the first day. On the other hand, at the inland wells, there was an abrupt increase in water level during recharge events that took much longer to decline (~1–2 weeks) (Fig. 6D, E). Water levels at all wells were primarily driven by changes in the bay water level on longer timescales with a maximum seasonal change 0.82 and 0.92 m in the marsh and deep wells respectively, 0.67 m for the middle well, and 0.96 and 0.65 m for inland well 1 and 2 respectively.

3.2.3. Specific conductance change (cross-correlation)

As there were no estimated overwashes for the marsh and deep wells, specific conductance in these wells was cross-correlated with estimated overwash from the middle well. Specific conductance was correlated

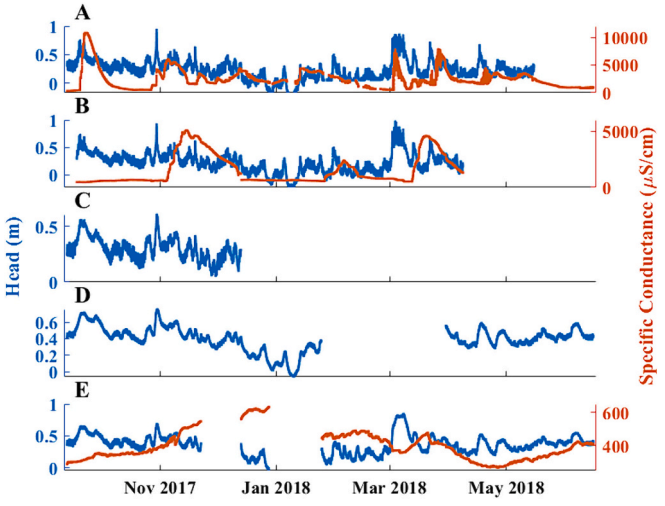

Fig. 5. Fire island hydraulic head and specific conductance data for A) Shallow marsh well, B) Deep marsh well, C) Middle well, D) Inland well 1, and E) Inland well 2.

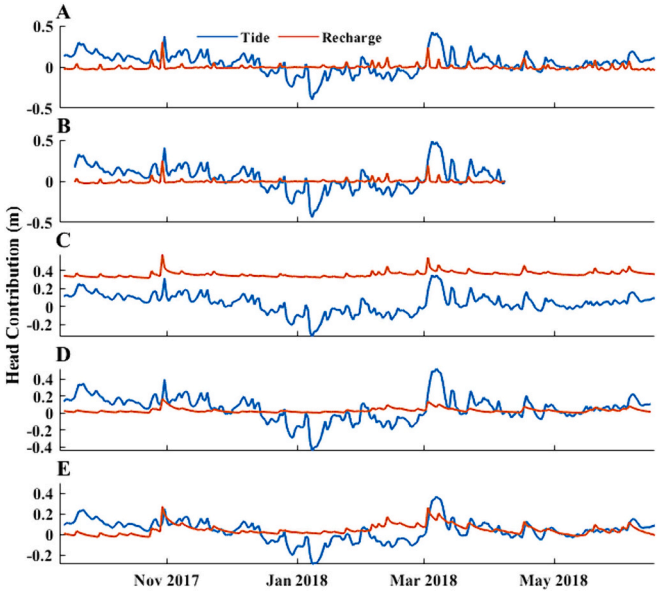

Fig. 6. Transfer function noise models for Fire Island, NY broken down by the influence of each hydrologic driver; major drivers bay level and recharge are shown for A) Marsh well, B) Deep marsh well, C) Middle well, D) Inland well 1, and E) Inland well 2.

with overwash at 10 % at a lag of 45 min and at 17 % for a lag of 22 days in the marsh well (Fig. 7A). The deep well showed a correlation of 20 % at a lag of 10 days (Fig. 7B). Thus, the deep well took a much longer time to experience salinization from an overwash event than the other two sites, likely due to lower hydraulic conductivity. The marsh and deep wells had a similar difference in depth to wells at Assateague but took longer to respond (10 days versus 8 days). Specific conductance in the marsh well was correlated with heads at 31 % at a 24-h lag (Fig. 7C), suggesting that heads rise at the wells before overwash occurs. Specific conductance in the deep well was correlated with heads at 46 % at a lag of 15 days (Fig. 7D). Thus, the response time for the deep well was longer for head-induced changes (~15 days) than for overwash-induced changes (~10 days).

3.3. Assateague Island, MD

3.3.1. Overview

Assateague experienced relatively frequent overwash, and water levels in all wells exhibited a similar response to overwash events (Fig. 8A–D). Because Assateague had a berm between the ocean and wells, when an overwash crested the berm, all the transect wells were inundated simultaneously. Generally, the water levels in well nest 3 were lower than those in well nest 2 and 1; however, during overwash events the water levels in well nest 3 substantially exceeded those in the other wells and this often persisted for long periods of time after an overwash event. This is opposite of what is expected, as the water-table overheight due to wave runup should cause water levels in well 3 to be higher than the inland wells. Additionally, this suggests that the flow direction changed relatively frequently with flow from ocean to bay occurring after overwash events and flow from bay to ocean occurring most other times.

Specific conductance increases coincided with overwash events, but showed more variability than water-level changes among wells (Fig. 8E–H). The shallow wells in each well nest transect generally had lower specific conductance than the deeper wells, demonstrating a typical island freshwater lens, except during overwash events when the specific conductance increased rapidly in the shallow wells before it was diluted by infiltrating precipitation. Specific conductance on Assateague

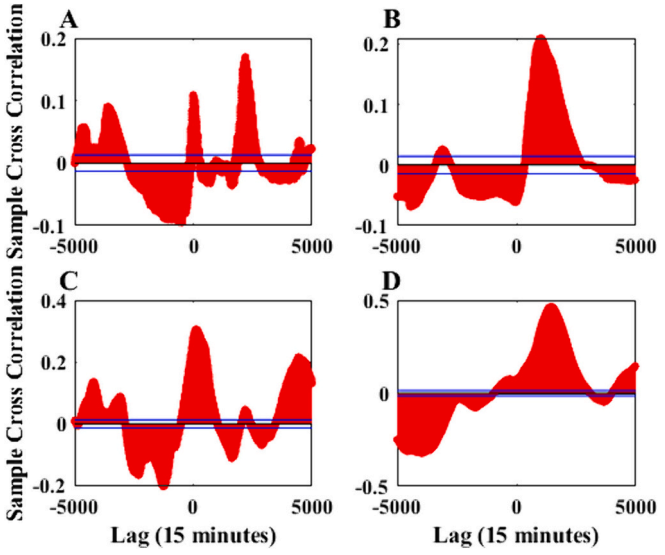

Fig. 7. Relationship between specific conductance, overwash, and head at lag times up to 52 days for Fire Island. Blue lines on plots indicated a p-value of <0.05 A) Correlation of specific conductance and overwash in the marsh well. B) Correlation of specific conductance and overwash in the deep marsh well. C) Correlation of specific conductance and head in the marsh well. D) Correlation of specific conductance and head in the deep marsh well.

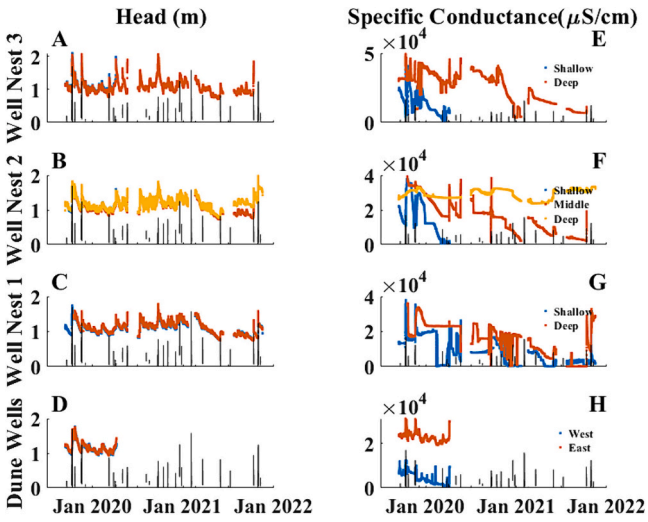

Fig. 8. Assateague Island hydraulic head and specific conductance data for each well nest. Black lines represent estimated overwash events in meters above land surface in A, C, E, and G, and are scaled by 10^4 on the right plots. A) Hydraulic head data for well nest 3. B) Specific conductance data for well nest 3. C) Hydraulic head data for well nest 2. D) Specific conductance data for well nest 2. E) Hydraulic head data for well nest 1. F) Specific conductance data for well nest 1. G) Hydraulic head data for dune wells. G) Specific conductance data for dune wells.

was highly dynamic and did not appear to have a stable average. Many of the wells started the monitoring period with relatively high specific conductance likely due to a storm-driven overwash that occurred just before the start of monitoring in September 2019. This was followed by a period of freshening until April 2020 when additional overwash increased specific conductance across the island. This elevated salinity was then flushed out gradually and reached a minimum in February 2021 when another large overwash spiked the specific conductance. This event was followed by another slow decline until October 2021. Not all predicted overwash events showed corresponding increases in salinity suggesting that there is likely substantial temporal change in overwash thresholds.

While generally all wells experienced specific conductance spikes at the same time, the sensitivity to and persistence of overwash-induced salinization varied among the well nests. Well 3 shallow had the most dynamic response to overwash events with specific conductance that rose rapidly and flushed out quickly after an overwash (Fig. 8E). For example, the overwash event on October 9th 2019 from Tropical Storm Melissa caused specific conductance to increase from ~11,000 μS/cm to 42,000 μS/cm and declined to 5,800 μS/cm by October 19th 2019. Well 3 deep also experienced rapid fluctuations due to overwash events with specific conductance spiking from ~30,000 μS/cm to ~48,000 μS/cm on October 9th 2019 returning back to 30,000 μS/cm by October 15th. Well nest 2 showed a similar pattern to well nest 3 with two discrete overwash events causing the specific conductance in the shallow well to increase to ~40,000 μS/cm for the first event and ~30,000 μS/cm for the second event (Fig. 8F). The duration of these spikes was much longer for the shallow well in well nest 2 than for the shallow well in nest 3 as the October 9th overwash took until November 13th (versus October 15th) to return to its pre-overwash specific conductance. Finally, the deep well in well nest 2 remained saline throughout the monitoring period (>50 % seawater salinity) and did not show any changes during overwash events suggesting that the freshwater lens was very shallow (approximately −2 m relative to NAVD88; Fig. 8F).

Well nest 1 experienced salinization from the same events as nests 2 and 3, but exhibited different flushing dynamics (Fig. 8G). Well 1 shallow began the monitoring period at ~15,000 μS/cm, and then experienced two overwash events that increased the specific

conductance to ~40,000 μS/cm. The events were extremely short-lived and the specific conductance returned to the initial value within 6 days. On the other hand, the specific conductance in well 1 deep took longer to increase, peaking about 12 days after the second overwash event and not returning to its previous baseline until over a month later.

The dune wells had less dynamic specific conductance fluctuations than the transect wells (Fig. 8H). The west dune well had a low specific conductance (<6,000 μS/cm) throughout the measurement period while the east well had a substantially higher specific conductance (~20,000 μS/cm). The west well experienced a freshening over the winter while the east well maintained a fairly constant specific conductance. Specific conductance spikes corresponded to some estimated overwash events, but generally these spikes are <10,000 μS/cm.

3.3.2. Water-level change (TFN model)

Water levels on Assateague were modeled using a combination of wave height, precipitation, evapotranspiration, tidal level, and overwash. All models showed that the ocean level, bay level, recharge, and overwash impact the head in the wells (Fig. 9). Model fits ranged from an R^2 of 0.70 for well 3 deep to 0.90 for well 2 shallow. Models with the best fit were those with the shortest water level time series, indicating that geomorphic change likely changes the influence of drivers over time. The ocean levels and bay levels generally exerted a moderate influence on the hydraulic head and changed gradually with average changes in the tidal level and average wave height. On the other hand, the water levels responded rapidly to precipitation and overwash events. Overwash played a stronger role in water level changes closer to the ocean and a lesser role closer to the bay. Water levels in the easternmost well nest had a response to overwash events that approached 0.6 m of head change over a single day (Fig. 9A). Similar spikes were observed for intense precipitation events. In July 2020, there was a 0.4 m increase in head due to recharge; however, this is likely due to overfitting as no overwash was predicted, but spikes in specific conductance suggest that an overwash occurred along with an intense precipitation event (Fig. 9B). The high hydraulic conductivity of the beach sand likely allowed both precipitation and overwash to rapidly change the water table elevation. The deeper wells in the transect experienced slightly less change in head due to overwash. For instance, on November 20th 2019, an overwash event caused water levels to rise 0.49 m in the well 3 shallow (Fig. 9A) versus 0.47 m in well 3 deep (Fig. 9B), 0.43 m in well 2 shallow (Fig. 9C) versus 0.23 m and 0.33 m in well 2 middle (Fig. 9D) and well 2 deep (Fig. 9E) respectively, and 0.24 m in well 1 shallow (Fig. 9F) versus 0.18 m in well 1 deep (Fig. 9G). Additionally, the impact of overwash decreased with distance from the ocean. The TFN models were unable to capture some of the high peaks in water level, likely due to uncertainties in the overwash estimates. The influence of tidal fluctuations also decreased with distance from the shore with well 3 experiencing a seasonal change of ~0.6 m (Fig. 9A) compared to ~0.2 in well 1 shallow (Fig. 9F). Ocean and tidal levels generally followed similar trends in all wells except for well 3 deep (Fig. 9B) and well 2 deep (Fig. 9E) which showed shorter-term (~2 days), low-amplitude fluctuations (<10 cm). In general, well 2 deep had higher-amplitude fluctuations likely indicating it is semi-confined and thus responds more rapidly to changes in ocean water levels (Fig. 9E). Recharge caused up to 0.42 m of head change across the island similar in magnitude to the impact of overwash.

3.3.3. Specific conductance change (cross-correlation)

The specific conductance changes at Assateague showed substantial cross-shore variability. Specific conductance changes in well nest 1 were correlated with overwash at lags of 1.75 days (Fig. 10A) and 8.6 days (Fig. 10B) for the shallow and deep wells, respectively, at approximately 12 %. Specific conductance was positively correlated with water levels for the shallow well with a lag of 1 h, and was negatively correlated with water levels for the deep well with a lag of 10 days. Well nest 2 showed different trends than well nest 1, with the shallow and deep wells being positively correlated with overwash at lags of 8.3 days (Fig. 10C) and 10.4 days (Fig. 10D). The middle well was positively correlated with

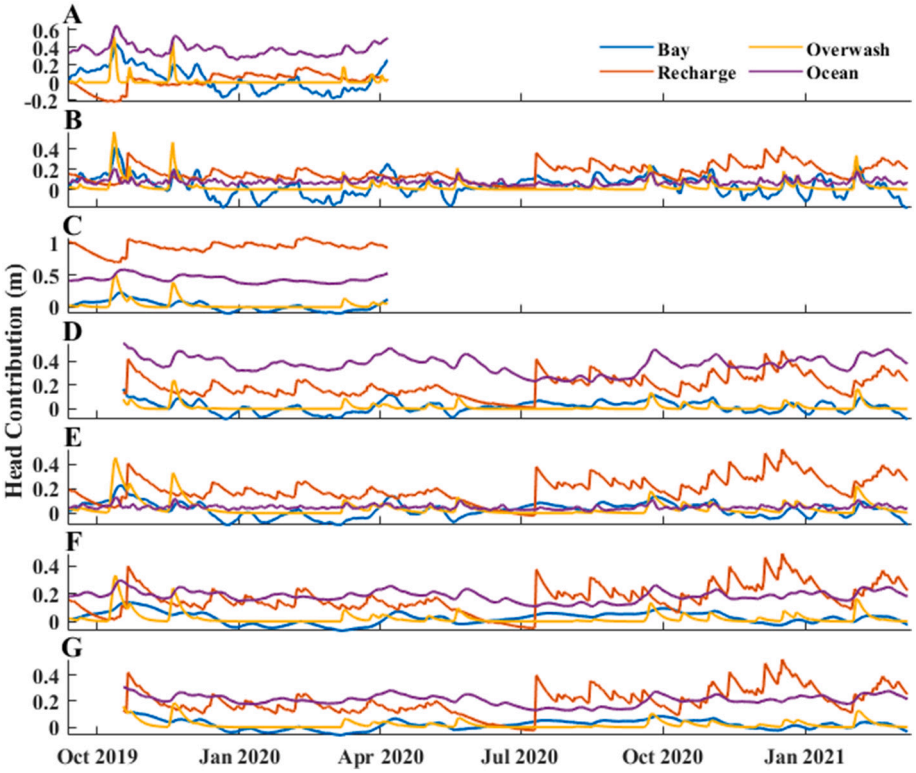

Fig. 9. Transfer function noise models for Assateague Island, MD broken down by the influence of each hydrologic driver including bay level, recharge, overwash, and ocean level A) Well 3 shallow, B) Well 3 deep, C) Well 2 shallow, D) Well 2 middle 1, E) Well 2 deep, F) Well 1 shallow, G) Well 1 deep.

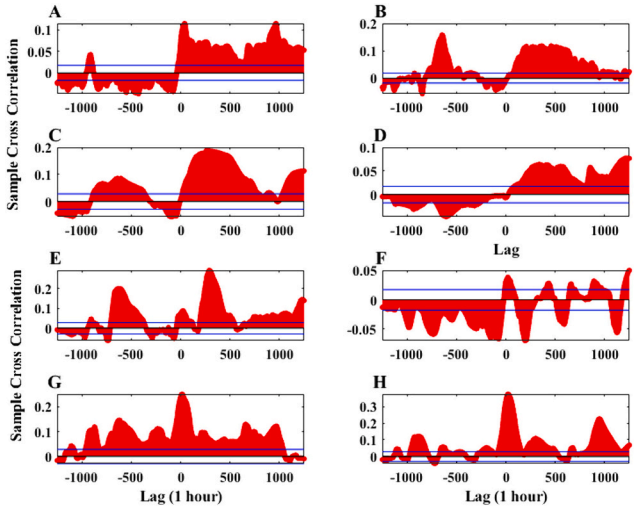

Fig. 10. Relationship between salinity and overwash at Assateague Island, MD A) Well 1 shallow, B) Well 1 deep, C) Well 2 shallow, D) Well 2 deep, E) Well 3 shallow, F) Well 3 deep, G) Dune well east, and F) Dune well west. Blue lines on plots indicated a p-value of <0.05.

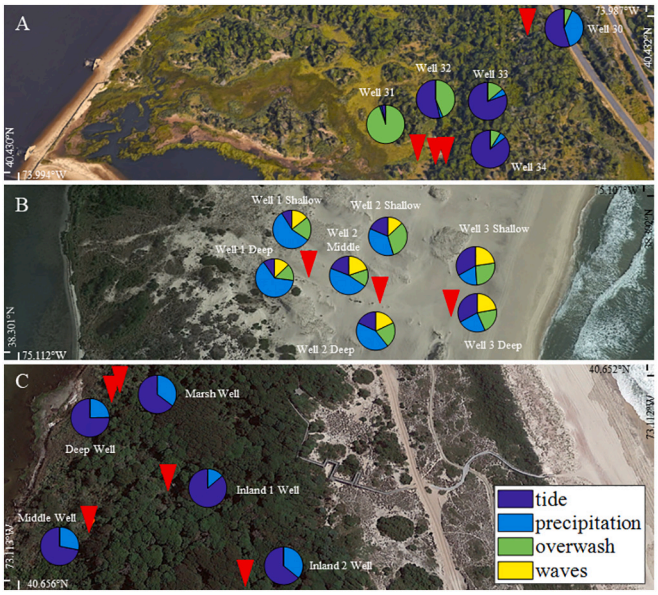

Fig. 11. Breakdown of primary drivers at each well on A) Sandy Hook, NJ B) Assateague Island, MD and C) Fire Island, NY.

overwash at all lags. Similarly, specific conductance was positively correlated with water level in the shallow and deep wells, but not correlated with water level in the middle well. Finally, well 3 shallow and deep both showed minimal correlation between specific conductance and overwash (Fig. 10E, F), but there was significant correlation between the water level and specific conductance in the shallow well. The dune wells exhibited the highest correlation between overwash events and specific conductance at 25 % and 37 % with lags of 13 and 19 h (Fig. 10G, H). This shows that specific conductance change was impacted by both overwash and water-level change, but the effects vary substantially from well to well. This is likely because complex flushing dynamics can temporarily change groundwater flow direction leading to less correlation between water levels and specific conductance.

4. Discussion

4.1. Drivers of water level change

4.1.1. Spatial variations in driver influence within sites

Groundwater levels at each site show spatial trends in the influence of the different drivers on water levels (Fig. 11A–C). The influence of precipitation/recharge increased with inland distance while the impact of overwash and tides declined with inland distance. At Fire Island and Sandy Hook, water level increases due to recharge/precipitation in the inland wells were greater than in the marsh wells (up to 0.2 m difference at Sandy Hook), and water levels took longer to decline (up to two weeks longer at Fire Island). Similarly, water levels on Sandy Hook and Assateague show larger impact of overwash closer to the shore and a lesser effect of overwash in the inland wells (0.9 m in well 31 versus 0.3 m in well 30 at Sandy Hook, and 0.6 m near the ocean versus 0.4 m near the bay at Assateague). The Sandy Hook and Fire Island wells displayed diurnal tidal fluctuations that declined in magnitude with distance from shore, while none of the Assateague wells showed an impact from diurnal tides. This agrees with other studies that observed a decline in diurnal tidal amplitude with distance from shore with diurnal tidal fluctuations only present within ~110 m of the shoreline (Abarca et al., 2013; Evans and Wilson, 2017). Similarly, all wells responded to seasonal changes in tidal levels with a range of 0.5–1 m of seasonal change which also depended on across-shore distance.

4.1.2. Variations in driver influence among sites

Groundwater levels at each site respond differently to the different drivers. The relative importance of each driver is impacted by the surface water connectivity, topography, and island geology. Surface water connectivity prevented some drivers from influencing water levels at some of the sites. For example, Assateague was most exposed to the ocean, and therefore was influenced by both ocean levels and wave heights (Fig. 11B). Sandy Hook, however, was more sheltered and therefore did not respond to ocean waves (Fig. 11A). Finally, the Fire Island wells were far from an inlet, so water levels were predominantly driven by bay levels and recharge (Fig. 11C). Topography plays a similar role in determining the influence of different drivers. Overwash at Sandy Hook had a more frequent impact on wells closer to the shore while overwash at Assateague occurred at all wells simultaneously because seawater was trapped in a surface depression. The Fire Island wells were topographically situated above most storm surges and therefore were not impacted by overwash. Finally, geology also played an important role in shaping the relative influence of different drivers. For example, Fire Island has a relatively low hydraulic conductivity, which limits the volume of water that can infiltrate when overwash events occur while Assateague has a relatively high hydraulic conductivity and overwash increases water levels rapidly. Therefore, barrier islands with low conductivity are more protected from overwash induced water-level change as long as there are surface connections to drain the ponded water. While hydraulic conductivity can impact the water-level response to overwash, aquifer storativity (the volume of water released from storage per unit area of aquifer per unit decline in hydraulic head) also affects the dominance of drivers on water levels.

Water level variations differ among sites, likely due to differences in aquifer storage properties. Water levels in well nest 1 on Assateague (~150 m from the shoreline) do not show a measurable response to tidal fluctuations while water levels at inland well 2 on Fire Island (~150 m from shore) have ~0.05 m tidal response This suggests that the storativity at Assateague is much higher than at Fire Island. Both storativity and transmissivity are expected to impact the tidal signal-propagation distance (Huang et al., 2015). However, lower hydraulic conductivity should decrease the inland tidal amplitude, and Fire Island has a lower hydraulic conductivity than Assateague. Thus, the storativity at Fire Island must be substantially lower than at Assateague. As both of these aquifers are unconfined, their different soil textures (clean sand at Assateague versus more silt/clay at Fire Island) mean they have different Van Genuchten parameters which influences the specific yield

(Pozdniakov et al., 2019). Thus, the soil type governs the temporal influence of different water-level drivers on barrier islands. Similarly, the deepest well on Assateague responds much more rapidly to changes in the ocean water level suggesting it has a low storativity and is semi-confined. This suggests that a confining unit exists on Assateague likely due to marsh deposits from when sea levels were lower. The existence of semi-confined marsh deposits at Assateague match those found by Anderson Jr. (2002) and Evans and Wilson (2017) at other barrier island sites.

4.2. Drivers of specific conductance change

The primary driver of specific conductance change across all sites was overwash. Others have shown that overwash is one of the primary drivers of specific conductance dynamics in barrier islands (Holt et al., 2017; Anderson Jr., 2002; Anderson Jr. and Lauer, 2008), but here we demonstrated that the influence of overwash on specific conductance varies substantially among sites. At Sandy Hook, the effects of overwash were felt most severely in the marsh where frequent overwash caused an elevated specific conductance. These effects diminished with distance from the shore, but specific conductance still periodically spiked up to the tree line (although spikes at the tree line generally did not last for a long time). At Fire Island, overwash occurred rarely and affected only the marsh wells. However, these wells are generally fresh. Finally, on Assateague all the wells responded to wind-driven wave-induced overwash events. The specific conductance spikes driven by these events persist for a long time (up to 6 months). Persistently high specific conductance after overwash events was also observed by Huizer et al. (2017) in a sandy-beach aquifer and attributed to wind-driven wave overwash.

The different sites respond differently to overwash due to the surface-water connectivity, geomorphology, and aquifer properties. Surface-water connectivity is one of the primary drivers of vulnerability to overwash as it governs the surge height experienced by the island. Assateague has the most connected surface water of all sites and thus experiences the most severe impacts of overwash-driven salinization due to higher ocean waves. Sandy Hook is much more protected from waves than Assateague because it is on the bay side of the spit and is sheltered by a sand bar. Finally, Fire Island is the most protected from wind-driven waves because the wells are far from an inlet and the bay is not wide/deep enough to produce large waves and thus experiences the least salinization. Similarly, the geomorphology/topography of the barrier island governs the inland distance an overwash event can propagate inland and the volume of saline water that can be stored on the surface. For example, Assateague has a berm between the wells and the ocean, which traps overwash water on the island, preventing it from draining back to the ocean. This depression storage causes much more saltwater to infiltrate the aquifer (Yu et al., 2016). On the other hand, there are limited surface depressions to fill near both the Sandy Hook and Fire Island wells, which likely limits the amount of salt water that can infiltrate the aquifer. Other studies have shown that surface depressions on atolls slightly decrease the size of the freshwater lens compared to atolls without surface depressions (Chui and Terry, 2015). Additionally, surface depressions can impede groundwater salinization during storms by limiting storage space in the unsaturated zone, but allow for up to 10 times more salt storage in surface-water filled depressions than infiltrates into the subsurface over the course of the storm (Chui and Terry, 2015). Thus, infiltration of saline water lasts long after the storm ends (Chui and Terry, 2012). This could be one reason why the freshwater-saltwater interface on Assateague is much shallower than at Fire Island or Sandy Hook as much more saltwater is able to infiltrate into the subsurface.

Both hydraulic conductivity and storativity affect the vulnerability of aquifers to storm-surge driven salinization. Yang et al. (2018), showed that the hydraulic conductivity strongly impacts the flushing time and penetration depth of saltwater. This difference is clear when comparing observations on Fire Island and Assateague. Assateague has a higher storativity and hydraulic conductivity and therefore has a smaller freshwater lens. Assateague is more susceptible to storm surge overwash while Fire Island has a lower hydraulic conductivity and a lower storativity. The lower storativity allows for faster flushing after storm surge events and less saltwater intrusion from tidal fluctuations (Paldor et al., 2022). Specific conductance peaks on Fire Island likely do not reach seawater specific conductance because the low hydraulic conductivity and short time span of overwash events decreases the flux of saline water relative to Assateague. The persistence of saline water on Assateague could be driven by the low-hydraulic gradient because the high hydraulic conductivity. This causes the flushing time to be much longer by decreasing the groundwater velocity. Finally, the higher hydraulic conductivity on Assateague allows changes in ocean water to propagate further inland and leads to more temporal variation in the direction of the hydraulic gradient. After a storm event the groundwater flow direction moves from the ocean towards the bay, but after a few days to weeks the gradient reverses and flow moves from the bay towards the ocean. This likely causes a longer flushing time as saline water moves towards the bay then back towards the ocean.

At all sites, the groundwater specific conductance experiences minimal changes due to tidal fluctuations and no fluctuations due to changes in evapotranspiration. Evapotranspiration can lead to hyper-salinization in barrier island mangroves (Stringer et al., 2010); however, these barrier islands did not experience any observable salinization from evaporation. Minimal changes were observed in the deeper freshwater-saltwater interface due to changes in ocean and bay water levels. This can be seen from well 2 deep on Assateague, well 34 on Sandy Hook, and the deep marsh well on Fire Island. This is in contrast to other studies which have observed fluctuations in atoll islands due to El Nino events and droughts (Oberle et al., 2017; Briggs et al., 2021) and fluctuations in an unconfined Mediterranean aquifer (Levanon et al., 2016, 2017). Few studies have been done with high resolution temporal data of specific conductance on a barrier island, so it is possible that differences in hydraulic properties drive the observed differences. Atoll islands tend to have a higher hydraulic conductivity than all of the islands observed in this study and therefore the interface is more likely to migrate tidally as the tidal signal can penetrate further. Specific conductance measurements at Sandy Hook suggest a small change in the interface location as the shallow wells 32 and 33 became saltier and the deeper well 34 slowly became fresher, although there are no detectable differences in drivers when these changes occur. The gradual freshening of the deeper well could be due to the formation of an upper saline plume which pushed the freshwater-saltwater interface deeper (Kuan et al., 2012) or geomorphological change causing changes to the groundwater discharge zones. Other evidence suggests there are temporal changes to the freshwater discharge zone. For example, well 31 shows correlation between specific conductance and overwash events sometimes, but at other times overwash occurs and the specific conductance does not change. This could be due to discharging water preventing infiltration of overwashing water. Cartwright et al. (2004) and Paldor and Michael (2021) also suggest based on modeling that the deeper Ghyben-Herzberg interface movement will occur due to storm surge water level change; however, we did not observe storm-surge induced temporal changes to the freshwater-saltwater interface at the two wells located in the interface (Assateague well 2 deep and Sandy Hook well 34). At Assateague, in well 1 shallow on May 20th 2020, we did observe an overwash event where specific conductance spiked rapidly in the shallow well and declined in the deep well likely due to the overwash pushing the shallow freshwater towards the deeper well.

4.3. Implications for ecosystems

Differences in drivers of groundwater level and specific conductance likely influence the distribution of ecosystems on barrier islands. Barrier islands have been shown to occupy one of two stable states: 1- low

elevation islands with frequent overwash and minimal diversity or 2-high-elevation vegetated islands with high diversity (Durán Vinent and Moore, 2015). While prior studies have focused on storm height and recurrence time (Durán and Moore, 2013), few studies have examined the role of groundwater levels on barrier island ecosystems. The northern part of Assateague, where our study was conducted, falls into the first typology and is barren due to the frequency and persistence of overwash events, which raise the specific conductance of the shallow groundwater and unsaturated zone. Roman and Nordstrom (1988) showed that vegetation communities correlated with the overwash frequency on Assateague. Fire Island falls into the second typology with high elevation and vegetation; however, it has experienced substantial recent changes in the vegetation composition (Raphael, 2014) that occurred after 2002 (Forrester et al., 2007). These changes are likely not driven by overwash-induced salinization as all wells are generally fresh with only limited specific conductance spikes in the marsh. Therefore, changes in ecosystem composition at Fire Island are more likely driven by rising water tables caused by sea-level rise. Similar to Fire Island, Sandy Hook is a high-elevation barrier spit with lots of vegetation; however, the forest on Sandy Hook has experienced less mortality than on Fire Island (Forrester et al., 2007). Sandy Hook water levels are less sensitive to bay water-level fluctuations than Fire Island, which could explain why the forest has not experienced the same declines. Additionally, the location of the water table influences the species that can grow. For instance, Sandy Hook is inundated frequently and stays wet, which permits marsh species to colonize, whereas Assateague dries quickly after storm events. Other studies have shown that different marsh species have different tolerances to elevation and anoxic conditions (Davy et al., 2011), with maximum root mass occurring with moderate inundation frequencies (Redelstein et al., 2018). This suggest that the presence of barren land is driven by whether there are species that can tolerate high variability in oxygen and salinity levels.

Important feedbacks exist between barrier island vegetation, geomorphology, and hydrology (Corenblit et al., 2015; Hacker et al., 2019; Miller, 2015), but more work is needed to quantify the feedbacks among these systems. While it is not possible to elucidate the direction of causation, these results suggest that differences in geomorphology impact the hydrology, which in turn impacts the ecology of barrier island systems. At Assateague, the maintenance of Ocean City Inlet is likely contributing to the overwash frequency and causing the island to migrate landward because it is preventing the alongshore movement of sediment (Leatherman, 1979). This impacts the vegetation community and prevents the island from transitioning to a vegetated, high-elevation state. Similarly, Fire Island has been experiencing erosion on the bay side as marsh elevation has not kept pace with sea-level rise (Roman et al., 2023). Lack of sediment accretion on Fire Island will likely shift the hydrological regime and thus impact the vegetation community; however, the effect of these geomorphic changes on the ecology requires further study.

While this study demonstrates differences in present-day vulnerability to overwash-driven salinization, it is not necessarily a good measure of future vulnerability. As storm-surge heights cross different thresholds the surface connectivity of barrier islands will change. If a storm surge can overtop a berm or dune and become trapped in a depression in the island there will be greater groundwater salinization. Similarly, given the lag between sea-level rise and barrier island retreat (Mariotti and Hein, 2022), low elevation islands like Assateague could be less vulnerable to drowning because they can migrate faster while Fire Island and Sandy Hook will likely have to experience increased forest mortality before they begin migrating. However, there must be sufficient sediment present for a barrier island to migrate which might exist for lower islands.

4.4. Limitations

Time-series models can be useful for identifying drivers of water-level change and salinization; however, these models incorporate some assumptions that must be considered. The TFN models are non-unique as there are different combinations of response functions and drivers that would provide similar model calibrations. Thus, the relative influence of the drivers might deviate from the results found in this study if different transfer functions were used. Additionally, all models were calibrated using the drivers we expected to have an impact on the water levels. Any important drivers that were left out could have an impact on the model calibration. Given that model fits had R^2 values ranging from 0.7 to 0.9, some of the TFN models were likely missing important drivers of water level change. Additionally, uncertainty in the input time series can lead to overfitting the model. The largest source of uncertainty in the input time series was likely overwash because sub-hourly wave-driven overwash was not accounted for in this study. Also, we observed that model fits were better for wells with shorter timeseries suggesting that geomorphological change alters overwash thresholds temporally. To better predict overwash events, a time varying estimation of the beach-face slope would be needed to better parameterize the wave runup and more frequent wave measurement would be necessary.

5. Conclusions

Using well data at three barrier islands along the mid-Atlantic US coast, we showed that drivers of barrier island groundwater level and specific conductance vary among islands and the relative influence of those drivers varies within individual islands. We observed that the influence of drivers varied spatially with recharge/precipitation increasing in impact with inland distance and overwash and tidal levels decreasing in impact. At Assateague, wave height was a critical driver of water level change, but was not a major driver at either Sandy Hook or Fire Island. Evapotranspiration had minimal impact across all sites. We also observed that barrier islands that would be expected to behave similarly due to similar geologic composition and climates demonstrate different characteristics due to hydrogeologic properties and geomorphologic connectivity. These differences have important implications for how barrier islands will evolve in the face of sea-level rise and more frequent storm surges. Sites with high connectivity to the ocean will likely face higher vulnerability to storm-surge overwash, as seen on Assateague, whereas sites with less surface connectivity will likely face higher vulnerability to increasing water tables due to sea-level rise, as seen on Fire Island.

CRediT authorship contribution statement

Ryan S. Frederiks: Writing – review & editing, Writing – original draft, Visualization, Validation, Methodology, Investigation, Formal analysis, Data curation, Conceptualization. **Anner Paldor:** Writing – review & editing, Methodology, Investigation, Data curation, Conceptualization. **Lauren Donati:** Writing – review & editing, Data curation, Conceptualization. **Glen Carleton:** Writing – review & editing, Funding acquisition, Data curation, Conceptualization. **Holly A. Michael:** Writing – review & editing, Validation, Supervision, Resources, Project administration, Investigation, Funding acquisition, Formal analysis, Conceptualization.

Declaration of competing interest

The authors declare that they have no known competing financial interests or personal relationships that could have appeared to influence the work reported in this paper.

Data availability

Data will be made available on request.

Acknowledgements

The authors would like to thank Christopher Lewis, Phillip Goodling, Lawrence Feinson, Brendan McCarthy and Amy Simonson at the U.S. Geological Survey for collecting much of the data used in this work and data QA/QC. The authors would also like to thank Brian Sturgis, Bill Hulslander, Jordan Raphael, and Kelsey Taylor from the National Park Service for facilitating site access. This project was funded by United States Geological Survey Water Resources Research Grant G19AP00005 and National Park Service grant P22AC00920. This material is based upon work supported by the University of Delaware Graduate College through the Unidel Distinguished Graduate Scholar Award. Any opinions, findings, and conclusions or recommendations expressed in this material are those of the authors.

References

Abarca, E., Karam, H., Hemond, H.F., Harvey, C.F., 2013. Transient groundwater dynamics in a coastal aquifer: The effects of tides, the lunar cycle, and the beach profile. Water Resour. Res. 49 (5), 2473–2488.

Allen, R.G., Pereira, L.S., Raes, D., Smith, M., 1998. Crop evapotranspiration—guidelines for computing crop water requirements—FAO. Irrigation and drainage paper 56, 15.

Anderson Jr., W. P. (2002). Aquifer Salinization from Storm Overwash. *Journal of Coastal Research, 18*(3), 413–420. JSTOR.

Anderson Jr., W.P., Lauer, R.M., 2008. The role of overwash in the evolution of mixing zone morphology within barrier islands. Hydrgeol. J. 16 (8), 1483–1495. https://doi.org/10.1007/s10040-008-0340-z.

Anthony Stallins, J., Corenblit, D., 2018. Interdependence of geomorphic and ecologic resilience properties in a geographic context. Geomorphology 305, 76–93. https://doi.org/10.1016/j.geomorph.2017.09.012.

Asaro, C., Nowak, J.T., Elledge, A., 2017. Why have southern pine beetle outbreaks declined in the southeastern U.S. with the expansion of intensive pine silviculture? A brief review of hypotheses. For. Ecol. Manage. 391, 338–348. https://doi.org/10.1016/j.foreco.2017.01.035.

Bakker, M., Schaars, F., 2019. Solving groundwater flow problems with time series analysis: You may not even need another model. Groundwater 57 (6), 826–833.

Befus, K.M., Barnard, P.L., Hoover, D.J., Finzi Hart, J.A., Voss, C.I., 2020. Increasing threat of coastal groundwater hazards from sea-level rise in California. Nat. Clim. Chang. 1–7 https://doi.org/10.1038/s41558-020-0874-1.

Bilskie, M.V., Hagen, S.C., Alizad, K., Medeiros, S.C., Passeri, D.L., Needham, H.F., Cox, A., 2016. Dynamic simulation and numerical analysis of hurricane storm surge under sea level rise with geomorphologic changes along the northern Gulf of Mexico. Earth's Future 4 (5), 177–193. https://doi.org/10.1002/2015EF000347.

Brakkee, E., Van Huijgevoort, Bartholomeus, R.P., 2022. Improved understanding of regional groundwater drought development through time series modelling: the 2018–2019 drought in the Netherlands. Hydrol. Earth Sys. Sci. 26 (3), 551–569.

Briggs, M.A., Cantelon, J.A., Kurylyk, B.L., Kulongoski, J.T., Mills, A., Lane, J.W., 2021. Small atoll fresh groundwater lenses respond to a combination of natural climatic cycles and human modified geology. Sci. Total Environ. 756, 143838 https://doi.org/10.1016/j.scitotenv.2020.143838.

Cardenas, M.B., Bennett, P.C., Zamora, P.B., Befus, K.M., Rodolfo, R.S., Cabria, H.B., Lapus, M.R., 2015. Devastation of aquifers from tsunami-like storm surge by Supertyphoon Haiyan. Geophys. Res. Lett. 42 (8), 2844–2851. https://doi.org/10.1002/2015GL063418.

Cartwright, N., Li, L., Nielsen, P., 2004. Response of the salt–freshwater interface in a coastal aquifer to a wave-induced groundwater pulse: field observations and modelling. Adv. Water Resour. 27 (3), 297–303. https://doi.org/10.1016/j.advwatres.2003.12.005.

Ceia, F.R., Patrício, J., Marques, J.C., Dias, J.A., 2010. Coastal vulnerability in barrier islands: the high risk areas of the ria Formosa (Portugal) system. Ocean & Coastal Management 53 (8), 478–486. https://doi.org/10.1016/j.ocecoaman.2010.06.004.

Chang, S.W., Chung, I.-M., Kim, M.-G., Tolera, M., Koh, G.-W., 2019. Application of GALDIT in assessing the seawater intrusion vulnerability of Jeju Island. South Korea. Water 11 (9), 1824. https://doi.org/10.3390/w11091824.

Chui, T.F.M., Terry, J.P., 2012. Modeling fresh water Lens damage and recovery on atolls after storm-wave Washover. Groundwater 50 (3), 412–420. https://doi.org/10.1111/j.1745-6584.2011.00860.x.

Chui, T.F.M., Terry, J.P., 2015. Groundwater salinisation on atoll islands after storm-surge flooding: modelling the influence of central topographic depressions: influence of topographic depressions on atoll groundwater salinisation after storm surge. Water Environ. J. 29 (3), 430–438. https://doi.org/10.1111/wej.12116.

Coastal Engineering Research Center, 1984. Shore Protection Manual. U.S, Army Corps of Engineers, Waterways Experiment Station, Vicksburg Mississippi.

Collenteur, R.A., Bakker, M., Caljé, R., Klop, S.A., Schaars, F., 2019. Pastas: open source software for the analysis of groundwater time series. Groundwater 57 (6), 877–885. https://doi.org/10.1111/gwat.12925.

Corenblit, D., Baas, A., Balke, T., Bouma, T., Fromard, F., Garófano-Gómez, V., González, E., Gurnell, A.M., Hortobágyi, B., Julien, F., Kim, D., Lambs, L., Stallins, J. A., Steiger, J., Tabacchi, E., Walcker, R., 2015. Engineer pioneer plants respond to and affect geomorphic constraints similarly along water–terrestrial interfaces worldwide. Glob. Ecol. Biogeogr. 24 (12), 1363–1376. https://doi.org/10.1111/geb.12373.

Davy, A.J., Brown, M.J.H., Mossman, H.L., Grant, A., 2011. Colonization of a newly developing salt marsh: disentangling independent effects of elevation and redox potential on halophytes. J. Ecol. 99 (6), 1350–1357. https://doi.org/10.1111/j.1365-2745.2011.01870.x.

Durán, O., Moore, L.J., 2013. Vegetation controls on the maximum size of coastal dunes. Proc. Natl. Acad. Sci. 110 (43), 17217–17222. https://doi.org/10.1073/pnas.1307580110.

Durán Vinent, O., Moore, L.J., 2015. Barrier island bistability induced by biophysical interactions. *Nature*. Climate Change 5 (2), Art. 2. https://doi.org/10.1038/nclimate2474.

Evans, T.B., Wilson, A.M., 2017. Submarine groundwater discharge and solute transport under a transgressive barrier island. J. Hydrol. 547, 97–110.

Forrester, J.A., Leopold, D.J., Art, H.W., 2007. Disturbance history and mortality patterns in a rare Atlantic Barrier Island maritime Holly Forest. Nat. Areas J. 27 (2), 169–182. https://doi.org/10.3375/0885-8608(2007)27[169:DHAMPI]2.0.CO;2.

Garner, A.J., Mann, M.E., Emanuel, K.A., Kopp, R.E., Lin, N., Alley, R.B., Horton, B.P., DeConto, R.M., Donnelly, J.P., Pollard, D., 2017. Impact of climate change on new York City's coastal flood hazard: increasing flood heights from the preindustrial to 2300 CE. Proc. Natl. Acad. Sci. 114 (45), 11861–11866. https://doi.org/10.1073/pnas.1703568114.

Hacker, S. D., Jay, K. R., Cohn, N., Goldstein, E. B., Hovenga, P. A., Itzkin, M., Moore, L. J., Mostow, R. S., Mullins, E. V., & Ruggiero, P. (2019). Species-Specific Functional Morphology of Four US Atlantic Coast Dune Grasses: Biogeographic Implications for Dune Shape and Coastal Protection. *Diversity*, *11*(5), Art. 5. doi:https://doi.org/10.3390/d11050082.

Holt, T., Seibert, S.L., Greskowiak, J., Freund, H., Massmann, G., 2017. Impact of storm tides and inundation frequency on water table salinity and vegetation on a juvenile barrier island. J. Hydrol. 554, 666–679. https://doi.org/10.1016/j.jhydrol.2017.09.014.

Housego, R., Raubenheimer, B., Elgar, S., Cross, S., Legner, C., Ryan, D., 2021. Coastal flooding generated by ocean wave- and surge-driven groundwater fluctuations on a sandy barrier island. J. Hydrol. 603, 126920 https://doi.org/10.1016/j.jhydrol.2021.126920.

Hoyt, J.H., 1967. Barrier Island formation. *GSA*. Bulletin 78 (9), 1125–1136. https://doi.org/10.1130/0016-7606(1967)78[1125:BIF]2.0.CO;2.

Huang, F.K., Chuang, M.H., Wang, G.S., Yeh, H.D., 2015. Tide-induced groundwater level fluctuation in a U-shaped coastal aquifer. J. Hydrol. 530, 291–305.

Huizer, S., Karaoulis, M.C., Oude Essink, G.H.P., Bierkens, M.F.P., 2017. Monitoring and simulation of salinity changes in response to tide and storm surges in a sandy coastal aquifer system. Water Resour. Res. 53 (8), 6487–6509. https://doi.org/10.1002/2016WR020339.

Illangasekare, T., Tyler, S. W., Clement, T. P., Villholth, K. G., Perera, A. P. G. R. L., Obeysekera, J., Gunatilaka, A., Panabokke, C. R., Hyndman, D. W., Cunningham, K. J., Kaluarachchi, J. J., Yeh, W. W.-G., Genuchten, M. T. van, & Jensen, K. (2006). Impacts of the 2004 tsunami on groundwater resources in Sri Lanka. Water Resour. Res., 42(5). doi:https://doi.org/10.1029/2006WR004876.

Irish, J.L., Frey, A.E., Rosati, J.D., Olivera, F., Dunkin, L.M., Kaihatu, J.M., Ferreira, C.M., Edge, B.L., 2010. Potential implications of global warming and barrier island degradation on future hurricane inundation, property damages, and population impacted. Ocean & Coastal Management 53 (10), 645–657. https://doi.org/10.1016/j.ocecoaman.2010.08.001.

Johnson, C.S., Miller, K.G., Browning, J.V., Kopp, R.E., Khan, N.S., Fan, Y., Horton, B.P., 2018. The role of sediment compaction and groundwater withdrawal in local sea-level rise, Sandy Hook, New Jersey, USA. Quater. Sci. Rev. 181, 30–42.

Kearney, W.S., Fernandes, A., Fagherazzi, S., 2019. Sea-level rise and storm surges structure coastal forests into persistence and regeneration niches. PloS One 14 (5), e0215977. https://doi.org/10.1371/journal.pone.0215977.

Kilheffer, C.R., Underwood, H.B., Raphael, J., Ries, L., Farrell, S., Leopold, D.J., 2019. Deer do not affect short-term rates of vegetation recovery in overwash fans on Fire Island after Hurricane Sandy. Ecol. Evol. 9 (20), 11742–11751.

Kuan, W.K., Jin, G., Xin, P., Robinson, C., Gibbes, B., Li, L., 2012. Tidal influence on seawater intrusion in unconfined coastal aquifers. Water Resour. Res. 48 (2) https://doi.org/10.1029/2011WR010678.

Leatherman, S.P., 1979. Migration of Assateague Island, Maryland, by inlet and overwash processes. Geology 7 (2), 104–107. https://doi.org/10.1130/0091-7613(1979)7<104:MOAIMB>2.0.CO;2.

Levanon, E., Shalev, E., Yechieli, Y., Gvirtzman, H., 2016. Fluctuations of fresh-saline water interface and of water table induced by sea tides in unconfined aquifers. Adv. Water Resour. 96, 34–42.

Levanon, E., Yechieli, Y., Gvirtzman, H., Shalev, E., 2017. Tide-induced fluctuations of salinity and groundwater level in unconfined aquifers – field measurements and numerical model. J. Hydrol. 551, 665–675. https://doi.org/10.1016/j.jhydrol.2016.12.045.

Lobo-Ferreira, J. P., Chachadi, A. G., Diamantino, C., & Henriques, M. J. (2005). Assessing aquifer vulnerability to seawater intrusion using Galdit method. Part 1: Application to the Portuguese aquifer of Monte Gordo. http://irgu.unigoa.ac.in/drs/handle/unigoa/1733.

Mahmoodzadeh, D., Karamouz, M., 2019. Seawater intrusion in heterogeneous coastal aquifers under flooding events. J. Hydrol. 568, 1118–1130. https://doi.org/10.1016/j.jhydrol.2018.11.012.

Mariotti, G., Hein, C.J., 2022. Lag in response of coastal barrier-island retreat to sea-level rise. Nat. Geosci. 15 (8), Art. 8. https://doi.org/10.1038/s41561-022-00980-9.

Masterson, J. P., Pope, J. P., Monti Jr., J., Nardi, M. R., Finkelstein, J. S., & McCoy, K. J. (2013). Hydrogeology and Hydrologic Conditions of the Northern Atlantic Coastal

Plain Aquifer System from Long Island, New York, (Report 2013–5133; Scientific Investigations Report, p. 88). USGS Publications Warehouse. doi:https://doi.org/10.3133/sir20135133.
Miller, T.E., 2015. Effects of disturbance on vegetation by sand accretion and erosion across coastal dune habitats on a barrier island. AoB PLANTS 7, plv003. https://doi.org/10.1093/aobpla/plv003.
Morgan, L.K., Werner, A.D., 2014. Seawater intrusion vulnerability indicators for freshwater lenses in strip islands. J. Hydrol. 508, 322–327. https://doi.org/10.1016/j.jhydrol.2013.11.002.
Oberle, F.K.J., Swarzenski, P.W., Storlazzi, C.D., 2017. Atoll groundwater movement and its response to climatic and sea-level fluctuations. Water 9 (9), 650. https://doi.org/10.3390/w9090650.
Otvos, E.G., 1981. Barrier Island formation through nearshore aggradation—stratigraphic and field evidence. Mar. Geol. 43 (3–4), 195–243. https://doi.org/10.1016/0025-3227(81)90181-X.
Otvos, E.G., Carter, G.A., 2013. Regressive and transgressive barrier islands on the north-Central Gulf Coast—contrasts in evolution, sediment delivery, and island vulnerability. Geomorphology 198, 1–19. https://doi.org/10.1016/j.geomorph.2013.05.015.
Paldor, A., Michael, H.A., 2021. Storm surges cause simultaneous salinization and freshening of coastal aquifers, exacerbated by climate change. Water Resour. Res. 57 (5) https://doi.org/10.1029/2020WR029213 e2020WR029213.
Paldor, A., Frederiks, R.S., Michael, H.A., 2022. Dynamic steady state in coastal aquifers is driven by multi-scale cyclical processes, controlled by aquifer Storativity. Geophys. Res. Lett. 49 (11) https://doi.org/10.1029/2022GL098599 e2022GL098599.
Pendleton, E.A., Williams, S.J., Thieler, E.R.. Coastal vulnerability assessment of Assateague Island National Seashore (ASIS) to sea-level rise. Open File Report 2004-1020. *US Geological Survey, Reston*. https://pubs.usgs.gov/of/2004/1020/html/cvi.htm.
Pendleton, E.A., Thieler, R.S., Williams, J., 2004b. Coastal vulnerability assessment of Fire Island National Seashore (FIIS) to sea level rise. USGS Open File Rep 03, 439.
Pendleton, E.A., Thieler, E.R., Williams, S.J., 2005. Coastal Vulnerability Assessment of Gateway National Recreation Area (GATE) to Sea-level Rise (No. 2004-1257). US Geological Survey.
Pozdniakov, S.P., Wang, P., Lekhov, V.A., 2019. An approximate model for predicting the specific yield under periodic water table oscillations. Water Resour. Res. 55 (7), 6185–6197.
Rahimi, R., Tavakol-Davani, H., Graves, C., Gomez, A., & Fazel Valipour, M. (2020). Compound Inundation Impacts of Coastal Climate Change: Sea-Level Rise, Groundwater Rise, and Coastal Precipitation. *Water, 12*(10), Art. 10. doi:https://doi.org/10.3390/w12102776.
Raphael, J., 2014. 50 Years of Vegetation Change in a Holly Maritime Forest. M.S., Hofstra University. http://search.proquest.com/pqdt/docview/1654262477/abstract/EC8320ABAD234BC4PQ/1.
Redelstein, R., Dinter, T., Hertel, D., Leuschner, C., 2018. Effects of inundation, nutrient availability and plant species diversity on fine root mass and morphology across a saltmarsh flooding gradient. Frontiers. Plant Sci. 9. https://www.frontiersin.org/articles/10.3389/fpls.2018.00098.
Roman, C.T., Nordstrom, K.F., 1988. The effect of erosion rate on vegetation patterns of an east coast barrier island. Estuar. Coast. Shelf Sci. 26 (3), 233–242. https://doi.org/10.1016/0272-7714(88)90062-5.
Roman, C.T., Lynch, J.C., Cahoon, D.R., 2023. Twenty-Year Record of Salt Marsh Elevation Dynamics in Response to Sea-Level Rise and Storm-Driven Barrier Island Geomorphic Processes: Fire Island. Estuaries and Coasts, NY, USA. https://doi.org/10.1007/s12237-023-01234-6.
Rotzoll, K., & Fletcher, C. H. (2013). Assessment of groundwater inundation as a consequence of sea-level rise. *Nature Climate Change*, *3*(5), Art. 5. doi:https://doi.org/10.1038/nclimate1725.
Schubert, C., 2010. Analysis of the Shallow Groundwater Flow System at Fire Island National Seashore, Suffolk County, New York (No. 2009-5259). US Geological Survey.
Stallins, J.A., 2005. Stability domains in barrier island dune systems. Ecol. Complex. 2 (4), 410–430. https://doi.org/10.1016/j.ecocom.2005.04.011.
Stallins, J.A., Parker, A.J., 2003. The influence of complex systems interactions on Barrier Island dune vegetation pattern and process. Ann. Assoc. Am. Geogr. 93 (1), 13–29. https://doi.org/10.1111/1467-8306.93102.
Stone, G. W., Zhang, X., & Sheremet, A. (2005). The Role of Barrier Islands, Muddy Shelf and Reefs in Mitigating the Wave Field Along Coastal Louisiana. *Journal of Coastal Research*, 40–55. JSTOR.
Stalter, R., Heuser, J., 2015. Survival and growth of Ilex opaca following superstorm Sandy, Sandy Hook, New Jersey. Holly Soc. J. 33 (1), 3–9.
Stanford, S.D., Miller, K.G., Browning, J.V., 2015. Coreholes reveal glacial and postglacial history at Sandy Hook. Unearthing NJ 11 (1), 1–6.
Stockdon, H.F., Holman, R.A., Howd, P.A., Sallenger Jr., A.H., 2006. Empirical parameterization of setup, swash, and runup. Coast. Eng. 53 (7), 573–588.
Stringer, C.E., Rains, M.C., Kruse, S., Whigham, D., 2010. Controls on water levels and salinity in a Barrier Island mangrove, Indian River lagoon. Florida. Wetlands 30 (4), 725–734. https://doi.org/10.1007/s13157-010-0072-4.
Studholme, J., Fedorov, A.V., Gulev, S.K., Emanuel, K., Hodges, K., 2021. Poleward expansion of tropical cyclone latitudes in warming climates. Nat. Geosci. https://doi.org/10.1038/s41561-021-00859-1.
Stutz, M.L., Pilkey, O.H., 2001. A review of global Barrier Island distribution. J. Coast. Res. 15–22.
Tebaldi, C., Strauss, B.H., Zervas, C.E., 2012. Modelling sea level rise impacts on storm surges along US coasts. Environ. Res. Lett. 7 (1), 014032.
Tolliver, K.S., Martin, D.W., Young, D.R., 1997. Freshwater and saltwater flooding response for woody species common to barrier island swales. Wetlands 17 (1), 10–18. https://doi.org/10.1007/BF03160714.
Uwihirwe, J., Hrachowitz, M., Bogaard, T., 2022. Integration of observed and model-derived groundwater levels in landslide threshold models in Rwanda. Nat. Hazard. Earth Sys. Sci. 22 (5), 1723–1742.
van der Valk, A.G., Squires, L., Welling, C.H., 1994. Assessing the impacts of an increase in water level on wetland vegetation. Ecol. Appl. 4 (3), 525–534. https://doi.org/10.2307/1941954.
Werner, A.D., Ward, J.D., Morgan, L.K., Simmons, C.T., Robinson, N.I., Teubner, M.D., 2012. Vulnerability indicators of sea water intrusion. Groundwater 50 (1), 48–58. https://doi.org/10.1111/j.1745-6584.2011.00817.x.
Yang, J., Zhang, H., Yu, X., Graf, T., Michael, H.A., 2018. Impact of hydrogeological factors on groundwater salinization due to ocean-surge inundation. Adv. Water Resour. 111, 423–434. https://doi.org/10.1016/j.advwatres.2017.11.017.
Young, D.R., Erickson, D.L., Semones, S.W., 1994. Salinity and the small-scale distribution of three barrier island shrubs. Can. J. Bot. 72 (9), 1365–1372. https://doi.org/10.1139/b94-167.
Yu, X., Yang, J., Graf, T., Koneshloo, M., O'Neal, M.A., Michael, H.A., 2016. Impact of topography on groundwater salinization due to ocean surge inundation. Water Resour. Res. 52 (8), 5794–5812. https://doi.org/10.1002/2016WR018814.
Zhang, K., Leatherman, S., 2011. Barrier Island population along the U.S. Atlantic and gulf coasts. J. Coast. Res. 27 (2), 356–363. https://doi.org/10.2112/JCOASTRES-D-10-00126.1.
Zinnert, J. C., Shiflett, S. A., Via, S., Bissett, S., Dows, B., Manley, P., & Young, D. R. (2016). Spatial–Temporal Dynamics in Barrier Island Upland Vegetation: The Overlooked Coastal Landscape. Ecosystems, 19(4), 685–697. doi:https://doi.org/10.1007/s10021-016-9961-6.
Zinnert, J.C., Stallins, J.A., Brantley, S.T., Young, D.R., 2017. Crossing scales: the complexity of Barrier-Island processes for predicting future change. BioScience 67 (1), 39–52. https://doi.org/10.1093/biosci/biw154.
Zinnert, J.C., Via, S.M., Nettleton, B.P., Tuley, P.A., Moore, L.J., Stallins, J.A., 2019. Connectivity in coastal systems: barrier island vegetation influences upland migration in a changing climate. Glob. Chang. Biol. 25 (7), 2419–2430. https://doi.org/10.1111/gcb.14635.